

Combined Implicit or Explicit Integration Steps for Hybrid Simulation

Authors:

Mehdi Ahmadizadeh, University at Buffalo, NY, 14260 mehdia@buffalo.edu
Gilberto Mosqueda, University at Buffalo, NY, 14260 mosqueda@eng.buffalo.edu

ABSTRACT

Explicit integration procedures have been widely adapted and applied to hybrid simulations of the seismic response of structures due to their simplicity. However, these procedures are conditionally stable and require small time steps for stiff systems, or systems involving high-frequency modes. In this study, a combined implicit or explicit integrator is proposed to solve the equation of motion for hybrid simulations. In this method, command displacement predictions are determined to load the experimental substructures beyond the current step using explicit kinematics expressions. The displacement and force measurements are then used to iteratively correct the explicit displacement prediction within the numerical model until an implicit formulation is satisfied. An explicit solution is accepted only in time steps for which the iterative correction of displacement fails to convergence after maximum number of iterations. This procedure limits communication between the experimental substructures and the numerical integrator, thus it is well suited for networked applications of hybrid simulation. Numerical and experimental simulations demonstrate the effectiveness of this numerical integration scheme, especially in utilization of longer time steps, prevention of excitation of higher modes, and testing of stiff systems.

INTRODUCTION

The increasing need for experimental verification of the seismic performance of novel structural systems has resulted in highly sophisticated dynamic test procedures. Further, new design procedures, such as performance-based design, require better understanding and modeling of the behavior of structures and components well into their nonlinear response range. Hybrid simulation, including real-time dynamic testing of substructures, offers an efficient means for assessment of dynamic and possibly rate-dependent behavior of structural systems subjected to earthquake excitation. Real-time dynamic testing of substructures, which is a natural evolution of pseudo-dynamic test methods developed in past decades [1-4], may have significant advantages over a shaking table test in terms of cost, scale size, geometry, and required physical mass of structures and components that can be tested [5].

The path-dependent behavior of experimental specimens does not allow for the direct implementations of implicit integration procedures with iterations in a hybrid simulation. As a result, explicit procedures without the need for iterations have been very popular. Further, the command displacement sent to actuator in an explicit method directly reflects

the desired displacement of the current time step. Despite their simplicity and applicability to hybrid simulations, explicit methods are only conditionally stable. Extensive research has been dedicated to the development of unconditionally stable integration procedures that do not require iterative displacements on experimental substructures [6-9]. Such improvements are necessary for the extension of hybrid simulation to large structural systems that may have high frequency modes, or for distributed testing, where the small time step requirements of explicit procedures may not be practical.

Recently developed integration procedures with improved stability characteristics take advantage of the initial elastic stiffness matrix of the structure [6-13], which may be a good approximation if the nonlinear behavior is limited. One procedure introduced by Pan *et al.* [14] measures the instantaneous behavior of single-degree-of-freedom experimental substructures to estimate the tangent stiffness. Another group of procedures introduce feedback loops involving experimental substructures [3, 15-18]; these procedures need to impose iterative displacements or forces on the specimens, which greatly increases the communication between the numerical and experimental substructures. In addition, uni-directional convergence has not been verified for these procedures, which is important for prevention of unwanted displacement reversals that can damage the experimental specimens or erroneously dissipate energy.

In this paper, a new method for numerical integration is proposed, in which recent measurements are used to implement an iterative scheme numerically, without physical imposition of displacements on the experimental substructures. The command displacement is still determined based on an explicit Newmark's kinematics equation, which can remain unchanged if an implicit correction is not possible in a particular step. The effectiveness of this approach has been demonstrated through numerical and experimental simulations.

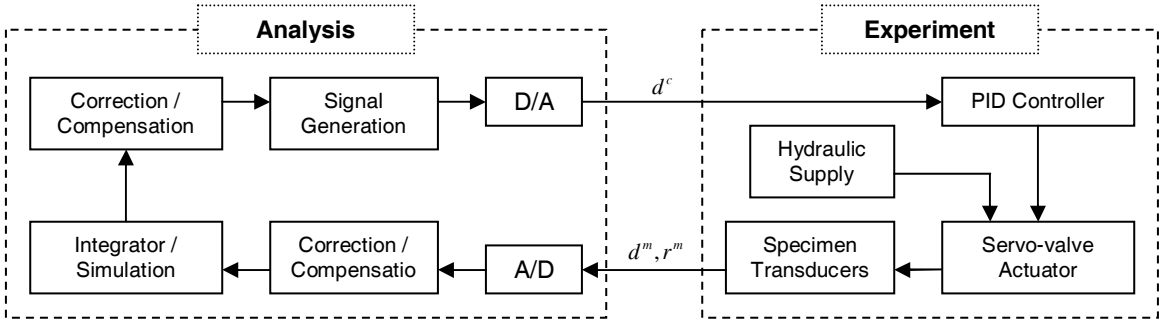

FIGURE 1
OVERALL BLOCK DIAGRAM OF A DISPLACEMENT CONTROLLED HYBRID SIMULATION

COMBINED IMPLICIT-EXPLICIT INTEGRATION SCHEME

In a displacement controlled hybrid simulation, the displacements computed by the numerical model are applied to the physical specimen, and resisting forces are measured and fed back into the numerical model, as shown in Figure 1. The essential components to a hybrid simulation include the numerical simulation component to solve the equation of motion for the hybrid model, an experimental setup, and the actuator and its control

system. Figure 1 also shows two correction and compensation blocks; one acting on the actuator command signals, and the other on the measurements. These blocks represent signal correctors and conditioners that are essential for stability and accuracy of any hybrid simulation [19].

In a hybrid simulation, the equation of motion of the combined numerical and experimental model can be expressed as:

$$\mathbf{Ma} + \mathbf{Cv} + \mathbf{Kd} + \mathbf{r} = -\mathbf{M}\boldsymbol{\iota}\ddot{u}_g \tag{1}$$

in which $\mathbf{M}$, $\mathbf{C}$ and $\mathbf{K}$ are mass, damping, and stiffness matrix of the system, $\boldsymbol{\iota}$ is the influence vector, $\mathbf{d}$, $\mathbf{v}$, and $\mathbf{a}$ are displacement, velocity and acceleration vectors, respectively; $\ddot{u}_g$ is the input ground acceleration and $\mathbf{r}$ is the restoring force measured in the experimental substructures, which may include strain-dependant, damping, or inertial forces.

The proposed method for solving the above equation of motion is first introduced through a modification of an explicit integration scheme for a single-degree-of-freedom system. The extension of this approach to multi-degree-of-freedom systems will be discussed later. In an explicit integration procedure, e.g. Newmark's method ($\beta = 0$, $\gamma = 1/2$), the command displacement is given by:

$$d_n^d = d_{n-1} + v_{n-1}\Delta t + a_{n-1}\frac{\Delta t^2}{2} \tag{2}$$

This displacement can be sent to the actuator as command displacement, after possible system delay and dynamics compensation. In this equation, step number is indicated by the subscripts for displacement, velocity and acceleration, and Δt is the integration time step. The measured force, r_n, corresponding to desired displacement d_n^d is then used directly to determine velocity and acceleration at step n, using the following relations:

$$a_n = \frac{1}{m + c\,\Delta t/2}\left(-m\,\ddot{u}_{g,n} - r_n - c\,v_{n-1} - c\,a_{n-1}\frac{\Delta t}{2}\right) \tag{3}$$

$$v_n = v_{n-1} + \frac{\Delta t}{2}\left(a_{n-1} + a_n\right) \tag{4}$$

In the above equation, it is assumed that all of the strain restoring force is originating from the experimental substructure, although the numerical stiffness term can be easily introduced. The next desired displacement d_{n+1}^d can then be determined using (2).

As shown above, the force corresponding to the imposed displacement is used without any modification. In the proposed approach, the measurements of force and displacement are used in an iterative scheme to correct the imposed displacement to satisfy the implicit form of Newmark's integration method. Here, the predictor displacement d_n^0 is taken to be the same as the previously determined desired displacement based on an explicit equation (d_n^d). With predictor velocity given by $v_{n+1}^0 = v_n + \Delta t\, a_n$, the objective is to solve the following equations iteratively:

$$\begin{aligned}
a_n^{i+1} &= \frac{1}{m}\left(-m\,\ddot{u}_{g,n} - r_n^i - c\,v_n^i\right) \\
v_n^{i+1} &= v_{n-1} + \Delta t\left[(1-\gamma)a_{n-1} + \gamma a_n^{i+1}\right] \\
d_n^{i+1} &= d_{n-1} + \Delta t\, v_{n-1} + \Delta t^2\left[\left(\frac{1}{2} - \beta\right)a_{n-1} + \beta a_n^{i+1}\right]
\end{aligned} \tag{5}$$

in which superscripts represent the iteration number, and β and γ are Newmark coefficients. The above equations are repeated until a convergence criterion is satisfied, such as:

$$\frac{\left(d_n^{i+1} - d_n^i\right)^2}{\left(d_n^{i+1}\right)^2} < \varepsilon \tag{6}$$

where ε is the convergence tolerance.

However, the challenge in solving the above relations is that imposing iterative displacements on experimental substructures is not acceptable in a hybrid simulation, as it may result in unrecoverable damage to experimental specimens and erroneous energy dissipation. Therefore, it is not advisable to measure experimental restoring forces, r_n^{i+1}, due to iterative displacements. In order to overcome this issue, recent data points are used to fit a second-order polynomial to both displacements and forces versus time. As shown in Figure 2, for experimental degrees of freedom, the iterative displacements are not physically imposed on the specimen. Instead, the displacement polynomial is used to estimate a time corresponding to that displacement and the corresponding force can then be determined by replacing the computed time into force polynomial. Therefore, the algorithm can be completed by addition of another step to the iterative scheme of (5), which estimates the restoring force r_n^{i+1} for the iterative displacement d_n^{i+1}. It is evident that the proposed approach does not require any additional communication between experimental and numerical subsystems, which is important for implementation in hybrid simulations with geographically distributed substructures.

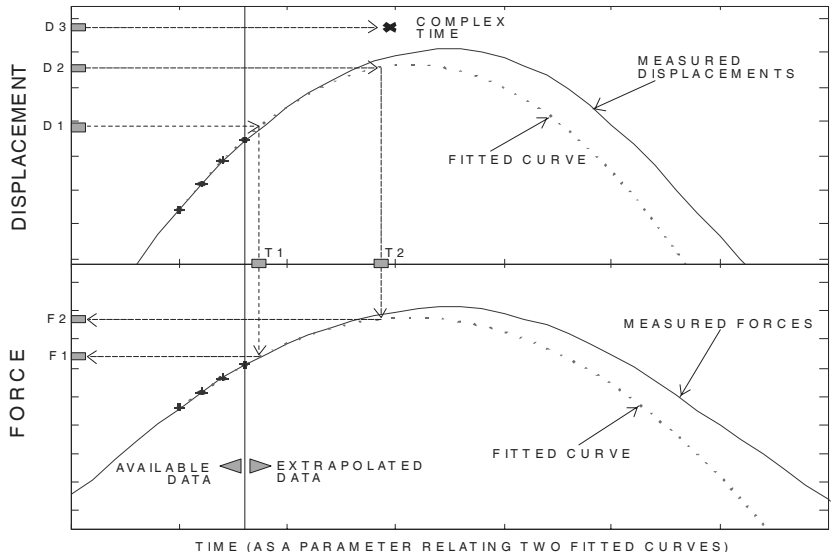

FIGURE 2
ESTIMATION OF FORCES CORRESPONDING TO ITERATIVE DISPLACEMENTS

Utilization of time as a parameter relating two fitted polynomials has several advantages. First, as the points are equally spaced in time, determination of fitted polynomial coefficients is computationally efficient. In addition, the time histories will always be of sufficient quality, as the effects of specimen nonlinearities will be less

pronounced on time histories compared to force-displacement curves. Clearly, the accuracy of fitted polynomials will decrease with distance from the fitted points. For this reason, one can impose limits on the variation of time within one step, in order to avoid extremely large extrapolations and ensure that the polynomials adequately represent the specimen behavior within the considered time step.

One problem in using this procedure occurs at displacement reversals when a real-valued time for the sought iterative displacement does not exist due to undershooting of displacements. Inserting the resulting complex-valued time in the fitted force polynomial results in a complex value; the real part of this value increases proportionally beyond the peak force, and the imaginary part is negligible, as long as the sought displacement remains close to the peak measured displacement. As a result, the absolute value of this complex number, which is very close to its real part, can be used as the estimated force. With this approach, the number of steps with successful completion of implicit integration increases, which has been observed to be advantageous for the overall accuracy of the simulation.

Compared to the operator-splitting method [8], this approach uses the measured data for iterations and eliminates the need for approximations using the initial stiffness matrix of the structure. However, as with most iterative schemes on non-linear systems, convergence is not guaranteed at each step due to noise and other experimental errors that can prevent accurate estimation of iterative forces. The failed iteration steps can be identified by detection of excessive time parameter variation or convergence failure after maximum number of iterations. As the presented procedure updates the states in the same way as an explicit procedure, it is proposed that the implicit correction be turned off in such situations. In other words, whenever force estimations of iterative displacements are not successful, or convergence cannot be achieved, the procedure switches to the explicit equations (3) and (4), which only use the last measurements to continue the simulation without interruption.

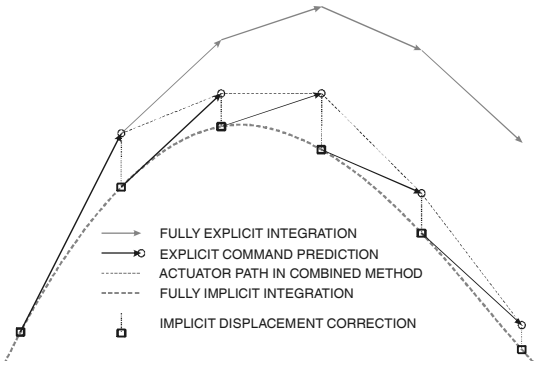

FIGURE 3
A SCHEMATIC DISPLACEMENT HISTORY OF COMBINED IMPLICIT-EXPLICIT INTEGRATION PROCEDURE

A schematic view of the performance of implicit or explicit integration method is shown in Figure 3. It is shown that the actuator follows the explicit desired displacement path, while an attempt is made to bring the displacement to the implicit equation result in the following step. Consequently, the actuator displacement will remain close to the results of an implicit scheme and numerical errors will not cumulate as much compared

to a fully explicit scheme. Of course, the actuator may not achieve the exact desired displacements as shown in Figure 3.

Extension to Multi-Degree-of-Freedom Systems Using α-Method

In order to improve the control of numerical damping in Newmark's Method, Hilber, Hughes, and Taylor introduced the α-Method [20]. In this approach, the time-discretized equation of motion and approximations of displacement and velocity are given by:

$$\begin{aligned} &\mathbf{M}\mathbf{a}_n + \mathbf{C}\mathbf{v}_n + \mathbf{K}\mathbf{d}_n + \alpha\left[\mathbf{C}\left(\mathbf{v}_n - \mathbf{v}_{n-1}\right) + \mathbf{K}\left(\mathbf{d}_n - \mathbf{d}_{n-1}\right)\right] = \mathbf{f}\left(t_n + \alpha\Delta t\right) \\ &\mathbf{d}_n = \mathbf{d}_{n-1} + \Delta t\,\mathbf{v}_{n-1} + \Delta t^2\left[\left(1/2-\beta\right)\mathbf{a}_{n-1} + \beta\mathbf{a}_n\right] \\ &\mathbf{v}_n = \mathbf{v}_{n-1} + \Delta t\left[\left(1-\gamma\right)\mathbf{a}_{n-1} + \gamma\mathbf{a}_n\right] \end{aligned} \tag{7}$$

The numerical damping in the algorithm can be controlled by parameter α, which when selected to be zero, reduces to Newmark's method (trapezoidal integration). If the parameters are selected such that $-1/3 \le \alpha \le 0$, $\gamma = \left(1-2\alpha\right)/2$, and $\beta = \left(1-\alpha\right)^2/4$, an unconditionally stable second-order accurate scheme results.

In a hybrid simulation, the force feedback from the experiment may include strain, damping, or inertial contributions; therefore, the time discrete equation of motion will be modified for a hybrid simulation as follows:

$$\begin{aligned} &\mathbf{M}^a\mathbf{a}_n + \mathbf{C}^a\mathbf{v}_n + \mathbf{K}^a\mathbf{d}_n + \mathbf{r}_n^e + \\ &\alpha\left[\mathbf{r}_n^e - \mathbf{r}_{n-1}^e - \mathbf{M}^e\left(\mathbf{a}_n - \mathbf{a}_{n-1}\right) + \mathbf{C}^a\left(\mathbf{v}_n - \mathbf{v}_{n-1}\right) + \mathbf{K}^a\left(\mathbf{d}_n - \mathbf{d}_{n-1}\right)\right] = \mathbf{f}\left(t_n + \alpha\Delta t\right) \end{aligned} \tag{8}$$

in which superscripts a and e denote analytical and experimental quantities, respectively. In order to ensure proper adaptation of this procedure to hybrid simulations, the inertial portion of the experimental restoring force should be removed from the increment multiplied by α. Therefore, the experimental mass should be known in order to solve this set of equations. The mass present in experimental substructures is generally small, although its accurate estimation is often possible through free vibration tests or direct measurements. In the combined integration procedure, step n corresponds to the step with predictor displacements given by:

$$\mathbf{d}_n^d = \mathbf{d}_{n-1} + \Delta t\,\mathbf{v}_{n-1} + \frac{\Delta t^2}{2}\mathbf{a}_{n-1} \tag{9}$$

As for the single-degree-of-freedom, (9) can be used to predict and command the displacement path of the actuator. The measured forces and displacements along the predicted traveled path are available for use in subsequent corrective iterations. The polynomials are then fitted to actuator feedback data, and used to estimate forces in the iterative scheme of (7) to update the states at step n. Therefore, in any integration step with iteration, the iterative displacements are determined in actuator coordinate system but they are not physically imposed on the specimen. Instead, following the same procedure described for single-degree-of-freedom systems, the forces corresponding to the iterative displacements are estimated.

As with most nonlinear analysis, convergance of the implicit scheme cannot be guaranteed in each step. Is this case, an explicit approach becomes necessary to continue the simulation. In the explicit steps, no polynomials will be fitted, and (7 and 8) should slightly change in order to use most recent measurements for improved accuracy. After imposition of predictor displacement, the experimental restoring force vector $\mathbf{r}_n^e$ becomes available, and the acceleration and velocity vectors are given by:

$$\mathbf{a}_n = \mathbf{A}^{-1}\left\{\mathbf{f}\left(t_n + \alpha\Delta t\right) - \begin{bmatrix} \mathbf{C}^a\left(\mathbf{v}_{n-1} + \frac{\Delta t}{2}\mathbf{a}_{n-1}\right) + \mathbf{K}^a\mathbf{d}_n + \mathbf{r}_n^e + \\ \alpha\left(\mathbf{M}^e\mathbf{a}_{n-1} + \frac{\Delta t}{2}\mathbf{C}^a\mathbf{a}_{n-1} + \mathbf{K}^a\left(\mathbf{d}_n - \mathbf{d}_{n-1}\right) + \mathbf{r}_n^e - \mathbf{r}_{n-1}^e\right) \end{bmatrix}\right\} \tag{10}$$

$$\mathbf{v}_n = \mathbf{v}_{n-1} + \frac{\Delta t}{2}\left(\mathbf{a}_{n-1} + \mathbf{a}_n\right) \tag{11}$$

where:

$$\mathbf{A} = \left(\mathbf{M}^a + \left(1+\alpha\right)\frac{\Delta t}{2}\mathbf{C}^a - \alpha\mathbf{M}^e\right) \tag{12}$$

can be evaluated prior to simulation.

It should be noted that the amount of mass in the experimental model should be modified if any event time scale other than unity is used (non-real-time fast hybrid simulation). As the inertia force generated by the experimental mass will be smaller for larger time scale values, the amount of experimental and analytical mass should be modified using the following relations:

$$\begin{aligned} \mathbf{M}^e &= \frac{\mathbf{M}^e_{\text{actual}}}{S_t^2} \\ \mathbf{M}^a &= \mathbf{M}^a_{\text{actual}} + \left(1 - \frac{1}{S_t^2}\right)\mathbf{M}^e_{\text{actual}} \end{aligned} \tag{13}$$

in which S_t is the simulation time scale. The above equation suggests that the effect of experimental mass quickly diminishes as the time scale increases. As an extreme case, the analytical mass should be equal to the total mass in a slow (pseudo-dynamic) hybrid simulation. A similar consideration should be taken into account for damping matrix, if the experimental model is known to show significant damping characteristics and the experiment is not real-time. If the damping matrix of the system is divided into analytical and experimental parts, as in:

$$\mathbf{C} = \mathbf{C}^a + \mathbf{C}^e \tag{14}$$

then the analytical part of damping matrix should be modified as:

$$\mathbf{C}^a = \mathbf{C}^a_{\text{actual}} + \left(1 - \frac{1}{S_t}\right)\mathbf{C}^e_{\text{actual}} \tag{15}$$

Clearly, if this rate dependent property of the experimental setup, $\mathbf{C}^e_{\text{actual}}$, is not well identified, then a real-time hybrid simulation ($S_t = 1$) is necessary for identification of damping characteristics.

Finally, it should be mentioned that in the above formulations, the numerical model is assumed to be linear; however, as the analytical stiffness matrix can be replaced by a tangential stiffness, this procedure does not have any limitation for extension to cases involving nonlinear numerical models.

Error Sources and Enhancements

As mentioned in the previous section, the major difference between this method and operator-splitting family of procedures adapted for hybrid simulation is that actual measurements are used to numerically satisfy (1) instead of imposing a single correction based on the initial stiffness matrix. It is expected that the proposed procedure will have better performance for highly nonlinear systems, in which tangential stiffness matrix

greatly differs from the initial value. However, this is only true if the fitted polynomials accurately represent the behavior of experimental substructures. As shown in Figure 2, the fitted polynomials follow the actual measurement as long as the extrapolation distance (variation of time parameter) is small. Therefore, it is important to limit the variation range of time within an iteration to ensure adequate correlation between the measurements and fitted polynomials.

From Figure 2 it is also evident that within the curve fitting range, the correlation between actual and fitted curves is very good. In the above-mentioned integration scheme, however, the final corrected displacement is expected to be close to the last point used for curve fitting. Consequently, the iterative displacements, which are expected to be close to the predicted displacement, can be either interpolated or extrapolated. In order to reduce the number of the cases in which extrapolation is necessary, one can make the actuator impose a displacement ahead of time by increasing the prediction time for determination of desired displacement, as in:

$$\mathbf{d}_n^d = \mathbf{d}_{n-1} + 2\Delta t \mathbf{v}_{n-1} + 2\Delta t^2 \mathbf{a}_{n-1} \tag{16}$$

By imposition of this displacement, the measurements will include data that are one step ahead of calculations, which makes interpolated force estimation possible for a larger number of iterative displacements. This modification is particularly useful for smaller values of time steps, where an increase of prediction distance will not significantly affect the accuracy of desired displacement. It is important to note that this change should not affect the initial iterative displacement vector, which should still be determined using (9). Several simulations have demonstrated that using (16) increases the number of integration steps with successful completion of iterative scheme.

As the fitted polynomials provide an instantaneous relation between the displacement of an actuator to its restoring force, this approach is very close to a complete implicit integration for single-degree-of-freedom substructures; however, when it comes to multi-degree-of-freedom experimental substructures, it does not consider the interaction of actuators. In other words, the effects of off-diagonal terms of tangent stiffness matrix of substructures are being neglected in displacement modification process after imposition of explicit displacement. Nonetheless, through numerical and experimental simulations, it has been observed that this simplification does not have any dramatic effect on the results.

Finally, it is recommended that a number of data points larger than the minimum required by the polynomial should be used in fitting process. As the data points are equally spaced in time, use of more data points will not significantly increase computational costs, but helps to reduce the effects of measurement noise in the fitted polynomials.

Delay Compensation

As with any other real-time hybrid simulation, delay issue should be properly addressed to ensure stability and accuracy. Delay compensation procedures that modify command displacement or force measurement signals can be used with this integration procedure. However, measured force correction procedure should equally modify the measured displacements, as their phase difference can result in unpredictable simulation performance from this integration approach.

In addition to polynomial extrapolation of command displacements, the same explicit expression for desired displacement can be used for delay compensation in command displacement signal. Therefore, (9) will result in the following expression for delay compensated displacement vector for j th actuator:

$$ {}^{j}\mathbf{d}_{n}^{c} = \mathbf{d}_{n-1} + \left(\Delta t + \tau_j\right)\mathbf{v}_{n-1} + \frac{\left(\Delta t + \tau_j\right)^2}{2}\mathbf{a}_{n-1} \tag{17} $$

in which τ_j is the j th actuator's delay. The command displacement for this actuator is then the result of transformation of the above displacement vector to actuator coordinates system.

NUMERICAL SIMULATIONS

Numerical models of hybrid simulation systems have significant advantages for performing low-cost computer simulations. These numerical evaluations are very useful for pre-test analyses, as well as development of new test procedures. One characteristic that makes these models very useful for performance evaluation of new procedures is that they provide the possibility of an 'exact' simulation by simply eliminating all uncertainty sources of the model associated with experiments. A direct comparison of the results will then give a full insight of the performance of the procedure in question. In this section, the results of numerical evaluation of the proposed integration procedure are presented. Several computer models have been used in this study, ranging from simple models with artificial error and delay sources to nonlinear actuator-specimen models.

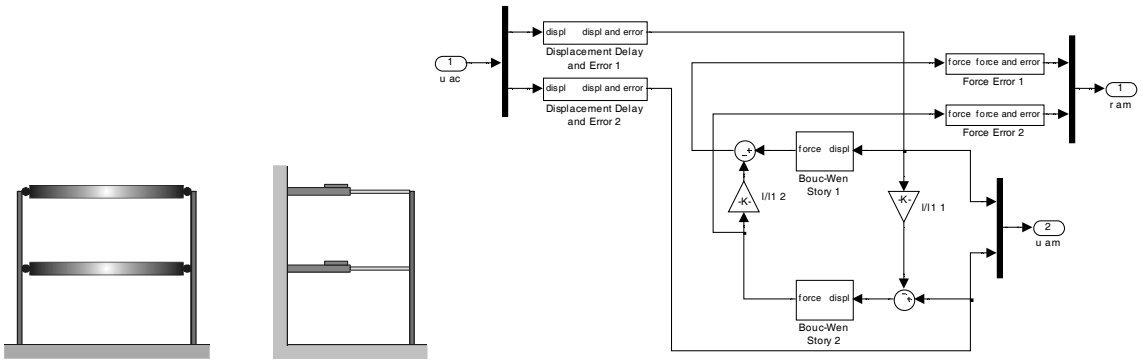

FIGURE 4
A TWO-DEGREE-OF-FREEDOM STRUCTURE AND CORRESPONDING LABORATORY SETUP FOR A COLUMN, AND CORRESPONDING SIMULINK MODEL

	Weight (kN)	Stiffness (kN/mm)	Yield Displacement (mm)
Story 2	44.5	0.95×2	5
Story 1	80.1	1.89×2	5

TABLE 1
STRUCTURAL PROPERTIES OF NUMERICAL TWO-DEGREE-OF-FREEDOM MODEL

The two-degree-of-freedom system of Figure 4 with properties listed in Table 1 is considered for a numerical study. The entire stiffness of the system is assumed to originate from the two-degree-of-freedom column setup. Damping is selected to be 5% of

critical, entirely considered in the analytical model. The majority of the mass is also assumed to be in the numerical model, but a small mass in experimental setup is always inevitable. The natural periods of this system are 0.60 and 0.15 seconds. The input excitation selected for these numerical simulations is the 1978 Tabas earthquake scaled in amplitude by 25%.

In order to simulate the actuator delay and noise in the measured signals, a Mathworks Simulink [21] model shown in Figure 4 is used. As illustrated, this model simulates the response of a two-degree-of-freedom substructure representing the two-story column of Figure 4, which is subjected to displacements imposed by two actuators. The restoring force is governed by two Bouc-Wen [22, 23] hysteretic models. The model carries out this simulation by artificially contaminating the measurements of displacement and force with the aid of several random sources. In addition, the imposition of displacement is delayed, where the amount of delay can be controlled by adjusting the means of random sources in the model multiplied by displacement increments. The amounts of actuator delay (12 and 8ms for lower and upper story actuators, respectively) and measurement noise have been selected based on actual experimental data and laboratory equipment information.

The simulation results using Central difference explicit integration scheme provide an unstable simulation with the response spuriously dominated by the second mode. The simulation stopped when the top story displacement exceeded the preset limit of 50mm. In this simulation, the experimental instrumentation sampling rate was 1024Hz, and a time step of 10/1024 seconds was used for integration.

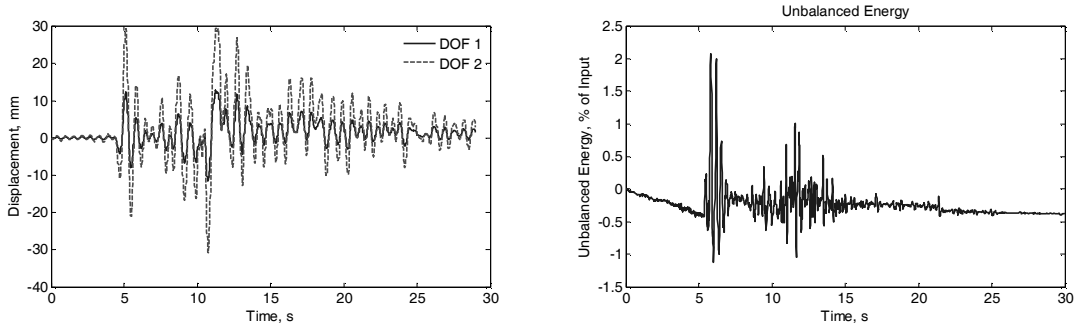

FIGURE 5
DISPLACEMENT HISTORY AND ENERGY BALANCE ERROR OF SIMULATION USING COMBINED INTEGRATION METHOD

Using the proposed integration scheme ($\alpha = 0$, $\beta = 1/4$, $\gamma = 1/2$) with combined implicit or explicit steps, the simulation is observed to have improved stability and accuracy. As shown in Figure 5, the simulation is stable, and the energy balance error shows minimal dispersion from zero, despite the existence of a relatively high-frequency mode in the system. The energy balance is defined here as the difference between the input earthquake energy and energy stored (kinetic and strain energy) or dissipated (hysteretic or viscous damping) by the structural model. The fact that energy error remains close to zero ensures that the equation of motion is solved accurately throughout the simulation. This energy error is a particularly useful measure of accuracy in actual experiments, where no exact simulation is available for direct comparison of results.

During this simulation, 88.2% of steps were successfully completed using the implicit approach, while the remainder of the steps remained explicit. The majority of the implicit steps require 1 to 4 iterations to converge, and only in a few cases the convergence is achieved after 5 iterations. In several implicit steps the convergence is bidirectional, and the physical imposition of iterative displacements may result in spurious energy dissipation in nonlinear specimens during reversals. The maximum number of iterations was set to 20, and the algorithm chooses to leave explicitly-determined states unchanged if convergence is not achieved within these iterations.

Effect of Experimental Mass Estimation Errors on Energy Balance

As mentioned in previous section, experimental mass matrix $\mathbf{M}^e$ is needed for utilization of α-method. It was also mentioned that the amount of mass in experimental setup is attempted to be as small as possible to reduce power requirements and achieve better actuator performance. Although estimation of experimental mass is generally possible with an acceptable accuracy, the developed numerical models have been used for a sensitivity analysis in order to observe the effects of errors in mass estimation.

As shown in Figure 6, two cases of two-degree-of-freedom simulation, in which the experimental mass are 1% and 5% of total mass, are considered. For each of these cases, experimental mass is slightly modified from its actual value, and overall energy balance of the system is considered. As shown, the alterations of energy balance are generally small, and more importantly, random. Therefore, one can conclude that the effects of experimental mass errors are small, comparable to the order of system randomness due to instrumentation noise and mistuning. However, this is only valid for small amounts of experimental mass, which is commonly the case in hybrid simulations. It should be mentioned that the effects of above-mentioned variations on displacement histories are insignificant.

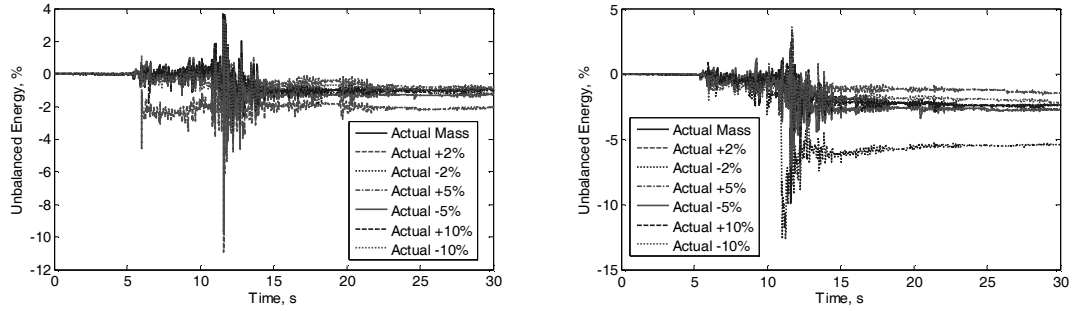

FIGURE 6
EFFECT OF MASS ESTIMATION ERROR ON THE OVERALL ENERGY BALANCE OF SYSTEM – LEFT: $\mathbf{M}^e = 0.01\mathbf{M}$, RIGHT: $\mathbf{M}^e = 0.05\mathbf{M}$

EXPERIMENTAL VERIFICATIONS

Single- and two-degree-of-freedom test setups are considered for experimental verification of the developed integration procedure, as shown in Figure 7. The test specimens consist of short elastic columns, which are mounted on clevises. The coupons inserted in clevises are designed to be weaker than the columns, and provide a nonlinear

response for evaluation of test procedures in nonlinear experiments, without damaging the columns during each test.

Single-Degree-of-Freedom Simulations

The natural period of the system has been selected to be 0.5 seconds. With a measured stiffness of about 880 N/mm, the required mass is 5.59 kN s/mm, out of which 0.012 kN s/mm is estimated to be present in the experimental specimen. The entire stiffness also originates from the experimental specimen, while the entire 5% of critical damping is taken into account in the numerical model. The setup was identified to include 16 milliseconds of delay, which is compensated using (17).

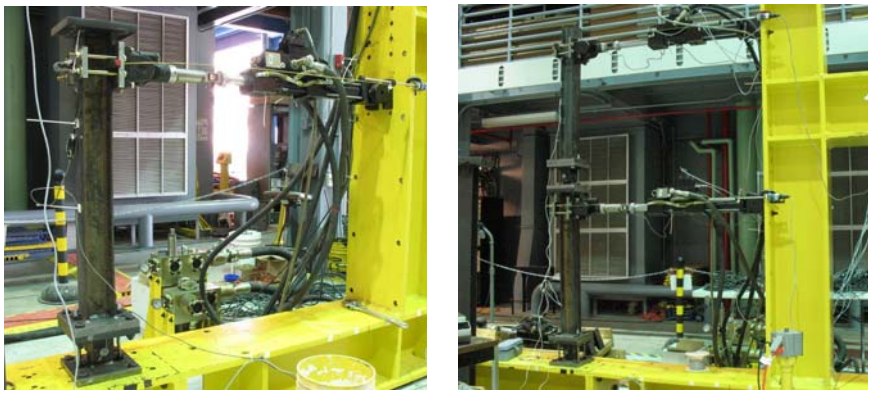

FIGURE 7
PICTURES OF SINGLE- AND TWO-DEGREE-OF-FREEDOM EXPERIMENTAL SETUPS

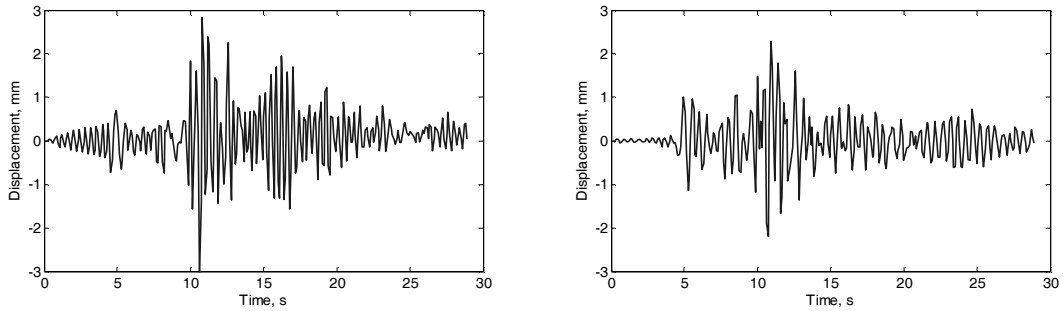

FIGURE 8
DISPLACEMENT HISTORY OF LINEAR EXPERIMENTAL SIMULATION 0.5-SECOND PERIOD SYSTEM WITH INCREASED INTEGRATION TIME STEP – LEFT: EXPLICIT CENTRAL DIFFERENCE, RIGHT: COMBINED IMPLICIT-EXPLICIT INTEGRATION

Explicit or combined implicit-explicit simulations of a single-degree-of-freedom system with a 1024Hz experiment sampling rate and a 10/1024-second integration time step do not show any significant difference, thus linear and nonlinear simulations can be carried out using both methods. In order to demonstrate the advantages of the proposed integration method, the experiment was repeated using a larger integration time step of 100/1024 seconds. The earthquake is also scaled down to 2.5% of the full record to ensure a linear response, thus providing similar responses in two experimental

simulations. As shown in Figure 8, while the result of explicit approach is on the verge of instability, the combined procedure has an acceptable accuracy, and more importantly remains stable, despite the large time step compared to the natural period of the system. In addition, the overall energy balance of the system is better maintained when the combined procedure is in use. Based on this observation, it can be concluded that the proposed approach shows significant improvement in terms of the selection of larger time steps, which is very beneficial for systems including high frequency modes and networked applications of hybrid simulation. In this test, 84.5% of the integration steps were successfully completed using implicit displacement corrections and state determination.

Two-Degree-of-Freedom Simulations

As shown in Figure 7, a two-degree-of-freedom setup has been built by mounting two single-degree-of-freedom setups as described in the previous section on top of each other. With two pairs of coupons in the lower clevis, and one pair in the upper one, static tests have been carried out for estimation of the stiffness matrix of the system:

$$\mathbf{K}^e = \begin{bmatrix} 4.86 & -1.41 \\ -1.41 & 0.68 \end{bmatrix} \text{kN/mm} \tag{18}$$

which is doubled to encompass both columns of a two-story structure as shown in Figure 4. The mass matrix is then selected in such a way that the natural periods of the system are 0.50 and 0.13 seconds. For comparison purposes, and to keep the specimens in linear range, two simulations with 2.5% of Tabas earthquake has been carried out, one with explicit central difference method, and the other with the proposed combined implicit-explicit integration. As shown in Figure 9, the explicit integration fails to remain stable, and results in the spurious excitation of the second mode of the system after a few seconds, while the proposed method is stable throughout the simulation.

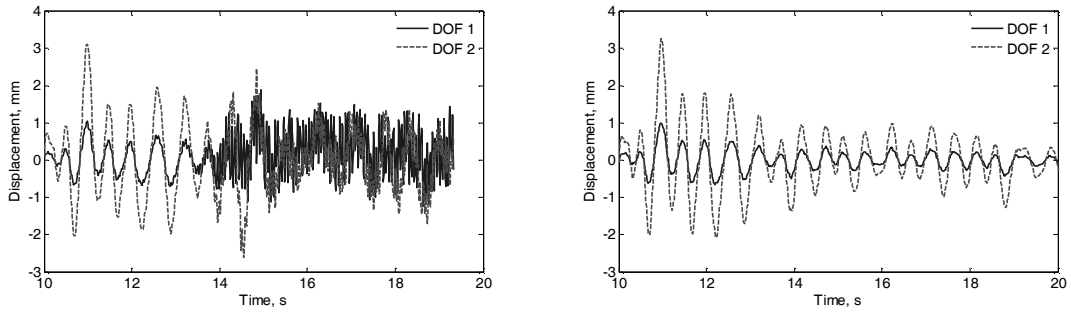

FIGURE 9
DISPLACEMENT HISTORY OF LINEAR EXPERIMENTAL SIMULATION OF TWO-DEGREE-OF-FREEDOM SYSTEM – LEFT: EXPLICIT CENTRAL DIFFERENCE, RIGHT: COMBINED IMPLICIT-EXPLICIT INTEGRATION

In order to demonstrate the effectiveness of the proposed integration method in nonlinear simulations, the internal forces have been increased by adding numerical mass and increasing earthquake scale factor. The displacement results of a two-degree-of-freedom system with natural periods of 0.60 and 0.15 under 20% of Tabas earthquake are shown in Figure 10. In this simulation, 87.1% of integration steps were successfully

completed with implicit corrections. Figure 10 also shows that the energy balance error remains close to zero during the simulation.

Another measure of accuracy is the hysteretic behavior of experimental substructure, compared to those observed by the numerical integrator. This comparison is shown in Figure 11 for the plastic hinge of the first story. The plastic hinge behavior is selected over the shearing behavior of columns due to the fact that the column in experimental setup is continuous past the first story, and hence, its behavior is essentially governed by bending and plastic hinge rotation rather than shearing of the column.

Figure 11 shows three different hysteretic plots for the first story plastic hinge. The actual hysteretic loop of the presumed plastic hinge in the first story of experimental substructure is simply a plot of measured forces versus measured displacements. The observed hysteretic loop is a plot of feedback forces, which are down-sampled at integration time step, versus desired displacements, which are explicit displacements started from converged displacements using (9); the desired displacement may be different from command displacements due to the implementation of delay compensation procedures. Finally, the converged hysteretic loops demonstrate the force and displacements at the end of implicit iterations. The similarity of these graphs shows that fitted polynomials have been successful in capturing the actual behavior of specimen, and the integration method does not add any significant contamination to the system.

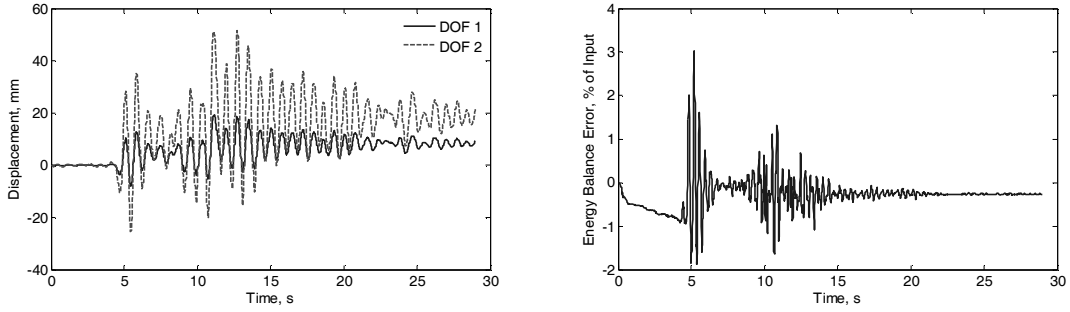

FIGURE 10
DISPLACEMENT HISTORY OF NONLINEAR EXPERIMENTAL SIMULATION OF TWO-DEGREE-OF-FREEDOM SYSTEM AND ITS ENERGY BALANCE

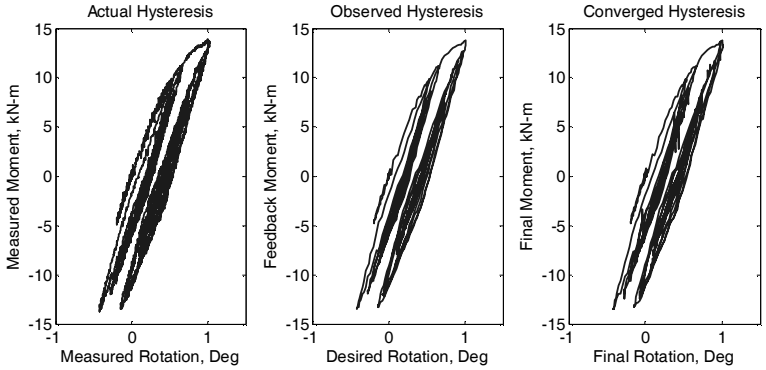

FIGURE 11
HYSTERETIC BEHAVIOR OF FIRST STORY PLASTIC HINGE

Experimental studies have also shown that the performance of the proposed integration scheme for small nonlinearities is comparable to what can be achieved using an operator-splitting method. However, this procedure does not utilize the initial stiffness matrix, and hence, is not restricted on the amount of nonlinearity in the system. In addition, it is not necessary to estimate the initial stiffness matrix of the system. Further experimental studies involving highly nonlinear experimental substructures are necessary for better comparisons of these two integration methods.

CONCLUSIONS

A new combined implicit-explicit integration scheme for real-time hybrid simulation has been proposed. The procedure uses measured forces and displacements in an iterative scheme, to eliminate the need for application of iterative displacements directly on experimental substructures. This method is closely comparable to a full implicit integration for single-degree-of-freedom substructures, while in multi-degree-of-freedom structures, the effect of off-diagonal terms of tangential stiffness matrix are ignored in the iterative scheme. However, through numerical simulations of multi-degree-of-freedom structures, it has been observed that the procedure has superior accuracy and stability compared to explicit integration methods.

The implicit integration scheme is modified such that the states are updated similar to an explicit Newmark procedure. Therefore, in cases that accurate estimation of forces corresponding to iterative displacements is not possible, the procedure automatically switches to the guaranteed-completion explicit scheme; i.e. the predicted displacement will remain unchanged, while the velocity and acceleration can be found using measurements corresponding to that displacement. Through numerical and experimental studies, it was observed that less noisy measurements can increase the percentage of implicit steps and improve simulation quality.

When α-method is used with the proposed integration scheme, the formulation requires the knowledge of experimental mass matrix. Although estimation of mass is normally possible with acceptable accuracy, it was observed that as long as the experimental mass is small, which is commonly the case in hybrid simulations, the simulation quality does not show a significant and meaningful dependency on estimation accuracy.

Compared to explicit procedures, the proposed approach was demonstrated to be able to eliminate spurious excitation of high frequency modes of the system. It was also observed that longer time steps can be utilized with this procedure, which can be useful for stiff systems, or networked applications of fast hybrid simulations. In addition, this integration method reduces the amount of required communications among numerical and experimental subsystems within an integration step, as the issuance of command displacements and acquisition of measurements occur only once within one integration step.

The fact that the proposed procedure does not need any initial estimation of system stiffness matrix makes it easier to use than operator-splitting series of integration methods. In addition, as the instantaneous behaviors of experimental substructures are captured through the use of measurements, the performance degradation is expected to be insignificant for highly nonlinear experimental substructures.

REFERENCES

[1] Mahin S.A. and Shing P.S.B. Pseudodynamic method for seismic testing. *Journal of Structural Engineering-ASCE*, 1985; Vol 111, No 7. pp. 1482-1503.
[2] Mahin S.A., Shing P.S.B., Thewalt C.R., and Hanson R.D. Pseudodynamic test method - current status and future directions. *Journal of Structural Engineering-ASCE*, 1989; Vol 115, No 8. pp. 2113-2128.
[3] Thewalt C.R. and Mahin S.A., *Hybrid solution techniques for generalized pseudodynamic testing (UCB/EERC-87/09).* 1987, University of California, Berkeley, Berkeley.
[4] Thewalt C.R. and Roman M. Performance parameters for pseudodynamic tests. *Journal of Structural Engineering -- ASCE*, 1994; Vol 120, No 9. pp. 2768-2781.
[5] Nakashima M. Development, potential, and limitations of real-time online (pseudo-dynamic) testing. *Philosophical Transactions of the Royal Society of London Series A-Mathematical Physical and Engineering Sciences*, 2001; Vol 359, No 1786. pp. 1851-1867.
[6] Chang S.Y. and Sung Y.C. *An enhanced explicit pseudodynamic algortihm with unconditional stability*. in *100th Anniversary Earthquake Conference*. 2006. San Francisco, CA.
[7] Chang S.Y., Tsai K.C., and Chen K.C. Improved time integration for pseudodynamic tests. *Earthquake Engineering & Structural Dynamics*, 1998; Vol 27, No 7. pp. 711-730.
[8] Nakashima M., Kaminoso T., Ishida M., and Kazuhiro A. *Integration techniques for substructure online test*. in *4th US National Conference of Earthquake Engineering*. 1990. Palm Springs, CA: Earthquake Engineering Research Institute.
[9] Wu B., Xu G., Wang Q., and Williams M.S. Operator-splitting method for real-time substructure testing. *Earthquake Engineering & Structural Dynamics*, 2006; Vol 35, No 3. pp. 293-314.
[10] Chang S.Y. Improved numerical dissipation for explicit methods in pseudodynamic tests. *Earthquake Engineering & Structural Dynamics*, 1997; Vol 26, No 9. pp. 917-929.
[11] Chang S.Y. Application of the momentum equations of motion to pseudo-dynamic testing. *Philosophical Transactions of The Royal Society of London Series A-Mathematical Physical And Engineering Sciences*, 2001; Vol 359, No 1786. pp. 1801-1827.
[12] Chang S.Y. Explicit pseudodynamic algorithm with unconditional stability. *Journal of Engineering Mechanics-ASCE*, 2002; Vol 128, No 9. pp. 935-947.
[13] Zhang Y.F., Sause R., Ricles J.A., and Naito C.J. Modified predictor-corrector numerical scheme for real-time pseudo dynamic tests using state-space formulation. *Earthquake Engineering & Structural Dynamics*, 2005; Vol 34, No 3. pp. 271-288.
[14] Pan P., Tada M., and Nakashima M. Online hybrid test by internet linkage of distributed test-analysis domains. *Earthquake Engineering & Structural Dynamics*, 2005; Vol 34, No 11. pp. 1407-1425.
[15] Bayer V., Dorka U.E., Fullekrug U., and Gschwilm J. On real-time pseudo-dynamic sub-structure testing: algorithm, numerical and experimental results. *Aerospace Science and Technology*, 2005; Vol 9, No 3. pp. 223-232.
[16] Shing P.B., Stavridis A., Wei Z., Stauffer E., Wallen R., and Jung R.Y. *Validation of a fast hybrid test system with substructure tests*. in *17th Analysis and Computation Specialty Conference*. 2006. St. Louis.
[17] Shing P.S.B. and Jung R.Y. *System dynamics in real-time pseudodynamic testing*. in *100th Anniversary Earthquake Conference*. 2006. San Francisco, CA.
[18] Shing P.S.B., Vannan M.T., and Cater E. Implicit time integration for pseudodynamic tests. *Earthquake Engineering & Structural Dynamics*, 1991; Vol 20, No 6. pp. 551-576.
[19] Ahmadizadeh M., Mosqueda G., and Reinhorn A.M. *Compensation of actuator delay and dynamics for real-time hybrid structural simulation*. in *4th World Conference on Structural Control and Health Monitoring*. 2006. San Diego, CA.
[20] Hilber H.M., Hughes T.J.R., and Taylor R.L. Improved numerical dissipation for time integration algorithms in structural dynamics. *Earthquake Engineering & Structural Dynamics*, 1977; Vol 5. pp. 283-292.
[21] *Simulink® Reference*. 1994-2006: The MathWorks® Inc, Natick, MA.
[22] Bouc R. *Forced vibration of mechanical systems with hysteresis*. in *4th Conference on Nonlinear Oscillations*. 1967. Prague, Czechoslovakia.
[23] Wen Y. Method for random vibration of hysteretic systems. *Journal of Engineering Mechanics*, 1976; Vol 102, No 2. pp. 249-263.